

1
2
3
4
5
6
7
8
9
10
11
12
13
14
15
16
17
18
19
20
21

REVISION 1

American Mineralogist Ms 5097

**Beyond the Equilibrium Paradigm:
How Consideration of Kinetics Enhances Metamorphic Interpretation**

WILLIAM D. CARLSON^{1,*}, DAVID R. M. PATTISON², MARK J. CADDICK³

¹Department of Geological Sciences, University of Texas at Austin, 2275 Speedway Stop C9000, Austin Texas
78712 USA

²Department of Geoscience, University of Calgary, Calgary, AB T2N 1N4, Canada

³Department of Geosciences, Virginia Tech, 4044 Derring Hall (0420), Blacksburg, VA 24060, USA

*Email: wcarlson@jsg.utexas.edu

Running title: Beyond the Equilibrium Paradigm

22 **Beyond the Equilibrium Paradigm:**
23 **How Consideration of Kinetics Enhances Metamorphic Interpretation**

24 **ABSTRACT**

25 The equilibrium model of prograde metamorphism, in which rocks are regarded as departing
26 only negligibly from equilibrium states as they recrystallize, has generated a wealth of petrologic
27 insights. But mounting evidence from diverse approaches and observations over a range of scales
28 has revealed that kinetic impediments to reaction may prevent metamorphic rocks from attaining
29 rock-wide chemical equilibrium along their prograde crystallization paths. To illustrate the
30 resulting potential for inaccurate interpretation if kinetic factors are disregarded, we briefly
31 review several case studies, including: out-of-sequence, metastable, and displaced isograds in
32 contact aureoles; paragenetic sequences documenting overstepped, disequilibrium reaction paths;
33 patterns of compositional zoning in garnet demonstrating partial chemical equilibrium;
34 petrologic incongruities between observation and thermodynamic prediction; and inhibited
35 reaction progress revealed by petrologically constrained numerical simulations of garnet
36 crystallization. While the equilibrium model provides an indispensable framework for the study
37 of metamorphic systems, these examples emphasize that all reactions require departures from
38 rock-wide equilibrium, so all rocks must traverse kinetically sensitive reaction paths during
39 recrystallization. Mindfulness of the potential significance of kinetic influences opens new
40 avenues for petrologic investigation, thereby enhancing both analysis and interpretation.

41 **Keywords:** kinetics, disequilibrium, crystallization, metamorphism

42 **INTRODUCTION**

43 The equilibrium paradigm—the concept that metamorphic rocks pass progressively
44 through sequential states of minimum free energy until they reach their thermal peak, remaining
45 steadily at equilibrium as they transform—has met with great success. It has allowed petrologists
46 to synthesize an abundance of accumulated observations into a coherent first-order picture of the
47 responses of earth materials to the heating and compression they experience in Earth's crust and
48 upper mantle. Increasingly, however, that view of metamorphism is being recognized as
49 incomplete, and in some cases misleading: it neglects the facts that reactions cannot proceed at
50 equilibrium and that metamorphic recrystallization involves passage through transient
51 disequilibrium states along a rock's reaction path.

52 Experiments have yielded significant insights into rate-limiting metamorphic processes
53 (e.g., Greenwood 1963; Walther and Wood 1984; review by Kerrick et al. 1991), and a rich
54 literature describes kinetically controlled processes due to retrogression or polymetamorphism.
55 In this article, we focus on the interpretation of natural samples traversing prograde paths,
56 emphasizing the ways in which kinetic impediments to reaction can produce crystallization under
57 conditions removed from the equilibrium state. We present observations spanning a range of
58 scales, diverse metamorphic environments, and varied analytical approaches (field and
59 petrographic studies, microchemical analysis, and thermodynamic and numerical modeling),
60 with the aim of highlighting the intrinsic value of considering from the outset the role of kinetics
61 in metamorphic interpretation.

62 **RATIONALE FOR THE EQUILIBRIUM VIEW OF METAMORPHISM**

63 The equilibrium model for prograde metamorphism has evolved as our understanding of
64 metamorphism has advanced. It originally focused on the idea that rocks attain their minimum
65 free-energy configuration at the maximum temperature they experience, giving rise to 'peak'

66 mineral assemblages and compositions. This interpretation is based on the metamorphic-facies
67 principle, which embodies predictable relationships between mineral assemblages and bulk
68 compositions, systematic associations of mineral assemblages in rocks of different bulk
69 composition metamorphosed together, and the repeatability of mineral assemblage sequences in
70 regional and contact settings the world over. Such regularity would be difficult to explain if
71 rocks did not approach their equilibrium configuration at their metamorphic peak.

72 This equilibrium model of metamorphism has permitted the full power of chemical
73 thermodynamics to be brought to bear on quantifying the conditions of metamorphism, resulting
74 in the development and widespread application of geothermobarometry. The subsequent
75 emergence of comprehensive thermodynamic databases and activity-composition models for
76 minerals, accompanied by phase-equilibrium modeling software, has permitted rock-
77 composition-specific phase diagrams to be calculated. These predict mineral modes and
78 compositions against which natural observations and measurements can be quantitatively
79 interpreted. Our current understanding of the range of metamorphic conditions in the crust and
80 mantle derives almost entirely from successful application of these methods.

81 The 'peak- T ' view of metamorphism is independent of both the tectonic path and
82 recrystallization mechanisms by which a given peak metamorphic mineral assemblage is
83 attained. Emphasis has increasingly moved to analysis of the pressure-temperature-time
84 evolution of metamorphic conditions, because it provides deeper insight into tectonic processes
85 and rates. In this context, an extension of the 'peak- T ' equilibrium model is that as rocks
86 progress along a path of changing pressure and temperature, they pass continuously through a
87 series of equilibrium states until peak temperature is reached. The implication is that the rate of

88 reaction is faster than the rate at which the P - T conditions change, so the rock is never far from
89 equilibrium at any point on its P - T path.

90 This version of the equilibrium model of metamorphism is more contentious. It ascribes the
91 modes and textures of mineral assemblages only to equilibrium reactions, even if achieved by a
92 series of interconnected local equilibria (e.g., Carmichael 1969), implying that kinetic barriers to
93 reaction are never significant. It neglects the specific mechanisms by which rocks recrystallize
94 and the rates at which that recrystallization occurs. On a P - T phase-diagram section, the
95 magnitude of the free-energy difference between competing phase configurations for a given P - T
96 condition, or between two different P - T conditions on either side of a modal-change line, is not
97 apparent. This energy difference is irrelevant to a purely equilibrium approach to metamorphism.
98 In natural processes, however, any equilibrium boundary must be overstepped to some degree to
99 proceed, and competing phase configurations might differ only slightly in free energy;
100 consequently, energetic barriers to recrystallization may potentially impede or delay the
101 attainment of the equilibrium configuration. In such cases, kinetically controlled processes may
102 then dominate the evolution of mineral assemblage and texture.

103 The petrologic community has widely adopted the calculation and description of P - T paths
104 of metamorphism, implying acceptance that certain rocks must contain stranded textural or
105 compositional remnants of their history. Recognition of preserved departure from rock-wide
106 equilibrium leads to two key petrological questions: What magnitude of departure from
107 equilibrium is possible, in terms of temperature and/or pressure, and more generally, free
108 energy? Does the possibility of kinetically controlled processes influence the way one interprets
109 a rock's textural and modal features in terms of its P - T path?

110 **EVIDENCE FOR THE IMPORTANCE OF KINETICS TO PETROLOGIC INTERPRETATION**

111 **Petrological evidence**

112 Classic examples of kinetic controls on metamorphic reaction progress include the
113 widespread co-existence of the Al_2SiO_5 polymorphs andalusite and sillimanite, and the
114 occurrence of locally eclogitized granulites in the Bergen Arcs in Norway, in which the
115 conversion of granulite to eclogite is restricted to localized zones of ingress of hydrous fluid that
116 catalyzed the reaction (Austrheim 1987). Of broader interest is whether kinetic barriers can give
117 rise to significant departures from equilibrium during prograde metamorphism of pelitic and
118 basic lithologies involving devolatilization reactions. There is increasing evidence suggesting
119 that they do, and below we discuss several examples, ranging from the map scale to the
120 microscale.

121 **Nelson aureole, British Columbia.** Figure 1a shows the distribution of mapped isograds in
122 carbonaceous argillaceous host rocks in the Nelson aureole in southeastern British Columbia,
123 whereas Figure 1b shows the predicted position of reaction isograds based upon an equilibrium
124 thermodynamic model (details provided in Pattison and Tinkham 2009). The two most
125 conspicuous differences are (1) the exceedingly narrow mapped garnet zone, compared to the
126 ~900 m-wide garnet zone that is predicted assuming equilibrium, and (2) the >1000 m-wide
127 mapped zone of co-existence of staurolite-only and staurolite+andalusite-bearing mineral
128 assemblages, compared to the <100 m-wide staurolite+andalusite zone predicted assuming
129 equilibrium. The estimated thermal overstepping of initial garnet growth was 30 °C, and of
130 staurolite consumption, 60-70 °C. Other differences include (3) the predicted consumption of
131 garnet downgrade of the first occurrence of sillimanite vs. the persistence and indeed growth of
132 garnet upgrade of the consumption of staurolite in the natural rocks, and (4) the persistence of
133 andalusite upgrade of the first appearance of sillimanite.

134 A simple explanation for these disparities relates to differences in the rate at which the
135 macroscopic driving force for reaction builds up as the equilibrium boundaries are overstepped
136 (Waters and Lovegrove 2002; Pattison and Tinkham 2009). This energy is needed to overcome
137 kinetic barriers to nucleation and growth. The macroscopic driving force for reaction is termed
138 reaction affinity (A), and is defined as the negative of the free energy difference between the
139 equilibrium state, where $A = 0$, and any other state of the system that is not in equilibrium, where
140 $A \neq 0$ (de Donder 1936; Prigogine and Defay 1954). In the specific situation involving
141 overstepping caused by lack of nucleation, reaction affinity can be taken as the Gibbs free energy
142 difference between the thermodynamically stable (but not-yet-crystallized) products and the
143 metastable reactants, either in the form of the precursor mineral assemblage (Pattison et al.
144 2011), or in the form of dissolved components in a supersaturated intergranular fluid (Carlson
145 2011). The rate of build-up of reaction affinity with respect to temperature overstep is a function
146 of the entropy change of the reaction (for overstep in pressure, it is the volume change). Figure 2
147 illustrates the rate of rise of reaction affinity with temperature overstep for some common
148 reactions in metapelites, with the slope of each line being the entropy change for the reaction,
149 which is strongly controlled by how much H₂O is released in the reaction. The reactions in the
150 Nelson aureole for which there is petrological evidence of overstepping are the low-entropy,
151 chlorite-free staurolite-to-andalusite reaction in the middle part of the aureole and, at lower
152 absolute temperatures at the outer edge of the aureole, the moderate-entropy chlorite-to-garnet
153 reaction.

154 An additional factor that likely played a role at this locality was the catalytic effect of fluid
155 (Rubie 1986). The clustering of the garnet, staurolite and andalusite isograds (Fig. 1a), combined
156 with textural evidence suggesting that all three porphyroblasts grew from reaction of fine-grained

157 matrix minerals, rather than involving the other porphyroblasts as predicted by equilibrium
158 thermodynamics, was interpreted by Pattison and Tinkham (2009) as a fluid-catalyzed cascade
159 effect triggered by introduction of H₂O to the grain-boundary network in response to the initial,
160 overstepped production of garnet within the stability field of staurolite and andalusite. A second
161 example of a fluid-catalyzing effect in the aureole is the local and patchy reaction of staurolite to
162 andalusite within a broad domain in which many rocks contain andalusite-free staurolite-bearing
163 assemblages, implying the existence of kinetic barriers to the conversion of staurolite to
164 andalusite that were locally lowered by fluid presence.

165 **Bushveld aureole, South Africa.** Metapelitic rocks in the Bushveld aureole, South Africa,
166 preserve a detailed microstructural record of an overlapping sequence of growth and
167 consumption of porphyroblasts of staurolite, andalusite, biotite and cordierite from a
168 chloritoid+chlorite-bearing precursor rock (Waters and Lovegrove 2002). The qualitative
169 paragenetic sequence the authors deduced from the microstructures is shown in Figure 3a. By
170 contrast, the predicted sequence of mineral growth and consumption, based on an equilibrium
171 phase diagram specific to the rock composition of interest, bears no resemblance to the observed
172 sequence whatsoever (Fig. 3b). The authors inferred that the reactions responsible for the
173 observed growth of the porphyroblasts were high-entropy muscovite+chlorite-consuming
174 devolatilization reactions that occurred in a narrow temperature interval up to 80 °C higher than
175 the low-entropy, weakly H₂O-producing chloritoid-consuming reactions predicted to initially
176 develop andalusite and staurolite (Fig. 3c). They concluded that the low-entropy reactions were
177 overstepped and ultimately overtaken in terms of reaction affinity by the high-entropy reactions,
178 at which point several reactions, both stable and metastable, occurred simultaneously, consuming
179 the chloritoid and producing the andalusite, staurolite and biotite now present in the rock.

180 A significant observation in this study was the recognition of the growth and consumption
181 of metastable cordierite within the reaction interval. Cordierite, stable at low pressures, should
182 not be present at the higher pressures of staurolite stability. Waters and Lovegrove (2002)
183 ascribed its development to its greater ease of nucleation compared to staurolite and andalusite.
184 A purely equilibrium interpretation of these rocks would require an implausible P - T path of
185 abruptly varying pressure. This example demonstrates that when P - T paths of metamorphism are
186 inferred from the sequence of growth and consumption of minerals, it may be necessary to
187 consider reactions other than those predicted in an equilibrium phase diagram, as also found in
188 experimental studies (e.g., Greenwood 1963). Whereas the final (peak) mineral assemblage in
189 the Bushveld rocks is consistent with that predicted assuming equilibrium, the path by which it
190 arrived at that assemblage was influenced by both the P - T path and the kinetically controlled
191 reaction path.

192 **Synthesis.** Pattison et al. (2011) provided other examples, mainly in metapelites, of regional
193 and contact localities showing thermal overstepping of reaction boundaries or a lack of
194 continuous equilibration during prograde metamorphism. Patterns emerge that can broadly be
195 grouped according to the entropy change of the reactions involved. The least amount of
196 demonstrable overstepping (5-30 °C) is observed for high-entropy devolatilization reactions,
197 especially chlorite-consuming reactions that occur over narrow multivariant intervals; the
198 greatest amount of overstepping (60-90 °C) is observed for low-entropy reactions, an observation
199 that pertains to reactions in both the greenschist and amphibolite facies; and intermediate degrees
200 of overstepping (30-70 °C) are inferred for moderate-entropy reactions, such as the chlorite-to-
201 garnet reaction (for which the upper end of the range is for Mn and/or Al-rich bulk compositions

202 in which the garnet-in reaction is predicted to occur at especially low temperatures, e.g., < ~450
203 °C).

204 **Additional factors.** Absolute temperature and heating rate influence some, but not all,
205 kinetically controlled processes, with lower temperatures and higher heating rates in general
206 favouring disequilibrium when reaction rates are controlled by surface and transport processes
207 (e.g., Putnis and McConnell 1980, section 6.2). However, in situations where disequilibrium is
208 due to delays in nucleation (e.g., Rubie 1998), heating rate is not the primary control on the
209 magnitude of the departure from equilibrium (Ridley and Thompson 1986; Waters and
210 Lovegrove 2002; Gaidies et al. 2011; Ketcham and Carlson 2012). The more important factor is
211 the magnitude of the temperature overstep, owing to the initial exponential dependence of
212 nucleation rate on reaction affinity (e.g., Ridley 1986). Other factors include the catalytic effects
213 of fluids (Rubie, 1986; see examples above) and the effects of deformation (e.g., Bell and
214 Hayward 1991), although the latter are less well understood.

215 **Implications for the metamorphic facies principle.** Whereas the above examples
216 demonstrate that the continuous-equilibrium model of prograde metamorphism may not always
217 pertain, do they constitute violations of the metamorphic-facies concept? In localities where
218 kinetic inhibitions to reaction have impeded crystallization of the thermodynamically stable
219 equilibrium assemblage, the answer must be yes. Nonetheless, they may not compromise the
220 broader principle. The examples noted in this article preferentially occur within individual facies
221 (e.g., greenschist facies, amphibolite facies), or between major reaction isograds (e.g., between
222 staurolite-in and K-feldspar-in isograds), rather than at the facies boundaries or major reaction
223 isograds themselves. The latter are typically marked by high-entropy devolatilization reactions
224 involving consumption of common hydrous minerals like chlorite and muscovite, in which the

225 amount of overstepping is expected to be minimal, or at least not sufficiently large to disrupt the
226 repeated patterns noted earlier. It may be that the metamorphic-facies principle succeeds because
227 it reflects major mineral-assemblage changes that occur at a few relatively discrete intervals
228 where significant reaction, recrystallization and chemical equilibration occur (Pattison et al.
229 2011). Whereas the broad features of a metamorphic sequence may be accounted for by an
230 equilibrium model, full understanding of the details of isograd patterns, mineral textures, mineral
231 modes, mineral compositions, and chemical zoning will likely require consideration of both
232 equilibrium and kinetics.

233 **Evidence from Mineral Zoning**

234 Metamorphic minerals that develop and preserve chemical zoning during growth can record
235 differences among elements in their length scales for chemical equilibration, signaling departures
236 from rock-wide equilibrium during prograde reaction. Achievement of chemical equilibrium
237 requires the elimination of all chemical potential gradients between reactants and products. The
238 length scales over which chemical equilibration can be established therefore depend on the
239 required transport distances and on the rates of diffusion through the intergranular medium. Both
240 may be expected to differ among chemical components involved in a reaction. When the length
241 scale for equilibration—that is, when the scale of *local equilibrium* in the sense of Thompson
242 (1959 and references therein)—varies significantly for different components, crystallization will
243 occur under conditions of *partial chemical equilibrium*, meaning system-wide equilibration for
244 some components, but not for others. Such conditions, imposed by the limitations of transport
245 kinetics in the intergranular medium, may be made particularly evident by growth zoning in
246 garnet.

247 For garnet and other aluminous porphyroblasts, the intergranular flux of Al is commonly
248 inferred to be rate-limiting for crystal growth (Carlson 2011), but all other garnet constituents
249 must also diffuse to the growing crystal from potentially different distal sources. Those elements
250 that diffuse more rapidly than Al will keep pace with growth, and the crystal's zoning will reflect
251 their negligible chemical-potential gradients in the form of near-equilibrium compositions at the
252 growth surface. Preservation of those compositions in the crystal's interior as reaction progresses
253 generates typical equilibrium growth zoning; an example would be bell-shaped profiles for Mn
254 in garnet. But elements that diffuse more slowly than Al cannot equilibrate over the required
255 length scale. As a result, their concentrations at the surface of growing garnet will be kinetically
256 controlled, and will be subject to a variety of influences that reflect the details of the reaction
257 path and mechanism.

258 A vivid example of partial chemical equilibrium in the form of 'overprint zoning' comes
259 from the study of Yang and Rivers (2001). The garnet crystal shown in Figure 4 exhibits smooth
260 concentric zoning for Mn, but a strongly banded distribution for Cr. Rapid intergranular
261 diffusion of Mn allowed equilibration over a length scale sufficient to flatten its chemical-
262 potential gradient, so that its zoning reflects progressive depletion of a spatially uniform, rock-
263 wide reservoir; in contrast, very restricted intergranular diffusion of Cr impeded its
264 redistribution, so that its zoning reflects *in situ* incorporation of the heterogeneous distribution
265 present in the precursor matrix. Figure 4 illustrates schematically the character of the chemical-
266 potential gradients involved, which reflect the relative rates of intergranular diffusion. Other
267 examples are less obvious, but no less profound in their consequences. Varied examples of
268 partial chemical equilibrium during prograde metamorphism are discussed in Carlson (2002) and
269 in Ague and Carlson (2013); here we sample just two more to illustrate the point.

270 The zoning of porphyroblasts in the garnet-zone metapelites of Harpswell Neck, Maine (cf.
271 Spear and Daniel 1998) highlights another instance in which a purely equilibrium-based
272 interpretation would be in error (Carlson et al. 2015, and references therein). As seen in Figure 5,
273 porphyroblasts that grew in locally quartz-rich, mica-poor environments (crystals A, B, C, with
274 quartz-rich layers identified by black zones in the Mg map) exhibit patchy overprint zoning for
275 Mn, Fe, and Mg, incorporating layering from the precursor; but for Ca and Y, these same crystals
276 display smooth concentric zoning, reflecting rock-wide equilibration. Equilibrium-based
277 interpretations, which require each isolated Mn high to originate in a separate nucleation event,
278 cannot be reconciled with the discrete central maxima for Y. In this instance, Ca and Y achieved
279 rock-wide equilibration, but Mn, Fe, and Mg did not. Raman spectroscopy of fluid inclusions
280 reveals that fluids attending early garnet growth were CO₂-rich; the difference in equilibration
281 for the various elements can be explained by their differential solubilities in such fluids.
282 Immediately adjacent crystals that grew in locally mica-rich environments (D) exhibit zoning
283 patterns little different from those expected from equilibrium prograde zoning, providing no clue
284 to the large variation in sizes of equilibration domains for different elements during their growth.
285 Such porphyroblasts falsely appear to mimic large-scale equilibrium crystallization, highlighting
286 the need for vigilance in interpretation.

287 Concentrations of trace elements, especially Y and the REEs, exhibit variability in garnet as
288 great or greater than that shown by major-element zoning. The data and recent synthesis of
289 Moore et al. (2013) revealed that Y+REEs may sometimes exhibit smooth zoning with
290 pronounced central peaks, demonstrating equilibration over long length scales with an
291 unchanging matrix assemblage (e.g. Otamendi et al. 2002), or they may exhibit a variety of
292 annular maxima, demonstrating equilibration, over similarly long length scales, with changing

293 accessory- or major-phase assemblages that are modulated by reactions occurring within the
294 matrix (e.g. Pyle and Spear 1999; Konrad-Schmolke et al. 2008). But Moore et al. (2013)
295 stressed that in other circumstances, these elements may express disequilibrium during garnet
296 growth, in the form of overprint zoning (Martin 2009), diffusion-limited uptake (e.g. Skora et al.
297 2006), or control by external fluids that did not equilibrate with the matrix mineral assemblage
298 (Moore et al. 2013). In all cases, the principal factor that determines the length scale for
299 equilibration is the rate of intergranular transport.

300 **Incongruities between calculated and observed phase equilibria**

301 Forward-modeled predictions of changing mineral composition with P and T commonly
302 yield detailed evidence of metamorphic peak conditions and of mineral growth along segments
303 of P - T paths (e.g. Konrad-Schmolke et al. 2007; Groppo et al. 2009). Set against this success in
304 recovering metamorphic conditions from mineral compositions, however, is a troubling
305 observation: zoned mineral compositions (most typically of garnet) may appear to track
306 equilibrium thermodynamic predictions of growth during burial and heating, but the
307 compositions of garnet calculated at the lowermost pressures and temperatures of its stability are
308 rarely seen in nature. Specifically, calculations that feature very low- T garnet stability suggest
309 that its Mn and Ca components should reach, or sometimes significantly exceed, 50 molar
310 percent (e.g., Caddick et al. 2010; Caddick and Kohn 2013). A rock-wide equilibrium response
311 would mandate the growth of Mn- and Ca-rich garnet (presumably to subsequently be preserved
312 as crystal cores), but natural crystals from mafic and pelitic lithologies are invariably far more
313 Fe- and Mg-rich. Scarce reports of extremely Mn- and Ca-rich low-temperature metamorphic
314 garnet (e.g., Tsujimori et al. 2006) imply that these compositions are indeed possible, countering
315 potential arguments that the available thermodynamic data are simply in error and leaving two

316 plausible interpretations: that early growth compositions are subsequently lost by
317 recrystallization or intracrystalline diffusion, or that garnet simply does not begin to grow at or
318 near the ‘garnet-in’ boundary in many cases.

319 An example of apparently delayed crystal growth comes from blueschist-facies rocks on
320 the Aegean island of Sifnos. Dragovic et al. (2012) isotopically dated multiple points from the
321 core to the rim of large garnet crystals, chosen to represent as much of the prograde metamorphic
322 history as possible. An equilibrium thermodynamic model constructed for the rock suggests that
323 the earliest-formed garnet preserves a composition appropriate for growth more than 1 GPa
324 deeper and/or 80 °C hotter than the interpreted point at which the ‘garnet-in’ reaction was
325 crossed (Fig. 6). Recent reinterpretation based upon an alternate model (Spear et al. 2014) also
326 yielded apparent garnet nucleation 70–90 °C hotter than the equilibrium garnet isograd, and
327 although the pre-garnet growth history is poorly constrained, any possible path to the point at
328 which garnet eventually grew reflects a similarly large overstepping of equilibrium garnet-
329 growth reactions. The large crystal size and relatively low maximum temperature of the sample
330 suggest that primary growth compositions are preserved without significant diffusive
331 modification, and repeatability of the observation in different Sifnos lithologies, including
332 samples that underwent 3-D tomographic analysis prior to thin sectioning (e.g., Dragovic et al. in
333 review), limits the chances of systematically failing to expose the true garnet core. It remains
334 most likely that initiation of garnet growth was delayed and that the total duration of crystal
335 growth was then brief (< 1 Myrs). In terms of free energy, the implied overstepping is similar in
336 magnitude to that inferred in other localities and lithologies, as described in the section that
337 follows. Recalculating the phase equilibria, but without permitting garnet stability, yields the
338 free-energy excess associated with deviation from equilibrium (Fig. 6), suggesting a reaction

339 affinity of ~ 0.5 kJ/mol of oxygen in garnet (6 kJ/mol of 12-oxygen garnet) at the P - T of inferred
340 initial garnet growth. The wide spacing of the affinity contours at low temperatures and pressures
341 reflects the fact that the reaction entropy and volume are small when close to equilibrium, so that
342 the driving force for metamorphic recrystallization remains insufficient to overcome barriers to
343 nucleation until a relatively large overstep in T and P is achieved.

344 As discussed previously, the phase diagram from which Figure 6 was constructed would
345 typically show only the state of minimum free energy. Quantifying the magnitude of the free-
346 energy departure associated with alternative configurations might prove to be a useful way in the
347 future of estimating the driving force for metamorphic recrystallization, and thus the likelihood
348 and magnitude of significant reaction overstepping (Pattison et al. 2011).

349 **Petrologically constrained numerical simulations of crystallization**

350 Numerical simulations—when carefully constrained by petrological observations and
351 measurements—can couple the kinetics of specific reaction mechanisms to the thermodynamic
352 driving forces for reaction in ways that permit quantitative estimation of the magnitudes of
353 departures from equilibrium during metamorphism. Depending upon which of the processes
354 essential to crystallization is regarded as rate-limiting, such models make qualitatively different
355 predictions for the reaction path: recent examples are those of Schwarz et al. (2011), Gaidies et
356 al. (2011), and Ketcham and Carlson (2012), for which the rate-limiting processes are,
357 respectively, reactant dissolution, product precipitation, and intergranular diffusional transport.
358 These models also differ in more subtle ways that influence their predicted departures from
359 equilibrium, and they have been assessed against different types of natural observations. The first
360 two models, those with no diffusional impediment to crystallization, predict smaller departures

361 from equilibrium than the third. Yet all of them highlight the importance to metamorphic
362 crystallization of a variety of kinetic factors and diverse potential reaction mechanisms.

363 Here we focus upon the diffusion-controlled model, because it has been applied by Kelly et
364 al. (2013a, 2013b) to garnet nucleation and growth in multiple samples that span a broad range of
365 *P-T* conditions, heating rates, and bulk compositions, as well as syn- to post-deformational
366 crystallization. This forward model provides a quantitative link between measureable textural
367 features in porphyroblastic rocks and the length scales of diffusion—and corresponding
368 departures from equilibrium—that generate them. For each sample, data from field, petrological
369 and microchemical analyses constrain a model *P-T-t* crystallization path, and thermodynamic
370 data yield the evolution of the free energy of reaction $\Delta_r G$ along it. Numerical simulation of
371 diffusion-controlled nucleation and growth then computes the sizes, locations, nucleation times,
372 and time-varying growth rates of porphyroblasts across the crystallization interval; factors
373 controlling nucleation rates and diffusional fluxes are adjusted to achieve quantitative
374 congruence with measured textural features in the modeled sample.

375 A typical outcome is shown in Figure 7. Key aspects are appreciable thermal overstepping
376 (27 °C) before the first nucleation event occurs, and a large departure from equilibrium (an
377 accumulation of 52 J·cm⁻³ of stored latent energy) before reaction rates accelerate sufficiently to
378 begin to reduce the reaction affinity. Nucleation is not restricted to a narrow interval barely
379 above the equilibrium temperature, as equilibrium-based models would require; instead, it
380 extends across nearly the entire crystallization interval, although it is concentrated around the
381 peak of overall metastability, as indicated by the maximum value of the latent energy of reaction.
382 This is confirmed by the observed variability of central Mn contents and their systematic relation
383 to crystal size, with cores of smaller crystals matching in composition the outer mantles of larger

384 crystals. Whereas the equilibrium model would require that all crystals nucleate on or near the
385 reaction boundary and thus acquire identical central compositions, the systematic variation in
386 measured central Mn contents instead documents that nucleation continues late into the
387 crystallization interval, so that many crystals nucleate well after the equilibrium boundary has
388 been crossed, and after much of the reaction has already taken place. The interval over which
389 reaction occurs spans a significant range of temperature and time: most crystallization (10-90%
390 of the total) takes place several tens of degrees (50-80 °C) above the equilibrium temperature,
391 and the bulk of the reaction occurs nearly ten million years after the equilibrium boundary is first
392 crossed. The modal proportion of garnet at any point in time and temperature is less—and in the
393 early stages of reaction, much less—than predicted by equilibrium phase diagrams, so changes in
394 effective bulk compositions are significantly delayed by the retardation of reaction progress.

395 The application by Kelly et al. (2013b) of such models to a suite of 13 diverse rocks yielded
396 consistent findings, paralleling those for the single example just described. The implication from
397 this modeling approach is that garnet crystallization may occur at conditions significantly
398 removed in temperature, time, and energy from the equilibrium state.

399 **CENTRAL CONCEPTS**

400 From the foregoing, four key concepts emerge.

401 First, in petrologic interpretation, the assumption of potentially significant kinetic influence
402 is less restrictive than the assumption of rock-wide equilibrium crystallization. The equilibrium
403 paradigm implies that one is justified in assuming that departures from the equilibrium state were
404 negligible during crystallization, unless and until evidence comes to light that requires otherwise.
405 But this assumption carries risk. As documented above, petrologically significant departures
406 from rock-wide equilibrium may occur during reaction, yet leave behind only subtle or cryptic

407 traces in the rock as the length scales for equilibration expand near the metamorphic peak. There
408 exists a continuum between obvious and cryptic instances of petrologically significant departures
409 from equilibrium during metamorphism; in the synthesis above, this is true regardless of the
410 scale of features examined, the environment of interest, or the investigative approach employed.
411 In terms of the processes involved, the clear-cut examples are not anomalous, nor substantively
412 different, from the examples in which only subtle indicators of disequilibrium survive. It may
413 therefore be limiting, and potentially misleading, to start from the expectation that equilibrium
414 has pertained throughout the metamorphic episode, and to abandon or modify that assumption
415 only when forced by some observation to do so. A less confining approach is to acknowledge
416 from the outset that all reactions require departures from equilibrium. Observations made with
417 this recognition in mind are more likely to capture the full range of features in the rock important
418 to petrologic interpretation.

419 Second, the *P-T-t* history and reaction path inferred from a rock on the basis of an
420 equilibrium model may be displaced substantially from the actual history and path. The onset of
421 reaction may be delayed, and eventual recrystallization may proceed too slowly for rock-wide
422 mineral assemblages, modes, and compositions to keep pace with changes in physical conditions.
423 Thus rocks may traverse reaction paths that are not predictable or interpretable from equilibrium
424 considerations alone.

425 Third, length scales for equilibration during metamorphic reaction may be decidedly
426 different for different elements under the same conditions, leading to partial chemical
427 equilibrium. That is, although local equilibrium may exist in systems that support large-scale
428 chemical-potential gradients, the length scale for such 'local' equilibrium may be different for
429 each chemical species. This requires explicit consideration of difficult questions: How do length

430 scales of equilibration differ among the major constituents of the minerals involved in a reaction,
431 and among minor/trace constituents? Which length scales are relevant and which are irrelevant to
432 any chosen petrologic interpretation?

433 Fourth, *P-T* paths inferred from mineral zoning, mineral modes, and even mineral
434 assemblages are vulnerable to error unless they are considered in the context of the potential for
435 partial chemical equilibrium and for kinetic impacts on reaction progress. Kinetic impediments
436 to equilibration may be more commonplace than is evident from the most obvious examples that
437 are readily accepted as indicative of metastability (e.g., the coexistence of polymorphs over
438 ranges of *P* and *T*), and these impediments can be of sufficient magnitude to alter zoning, modes,
439 and assemblages in ways that can compromise petrologic interpretation based on the equilibrium
440 model.

441 **LOOKING FORWARD**

442 It is a tribute to the power of the equilibrium paradigm that petrologists can now identify
443 and begin to quantify the departures from equilibrium that necessarily accompany metamorphic
444 crystallization. A pressing question, therefore, is how prevalent and how significant kinetic
445 controls on prograde metamorphic processes and products will prove to be. Are they important
446 yet often overlooked? The petrological community can address that issue by remaining mindful
447 of the possibility of kinetically influenced crystallization, in order to recognize evidence for it, to
448 capture the nuanced view of metamorphism that it provides, and to gain the enhanced insights
449 that it produces.

450 **ACKNOWLEDGEMENTS**

451 We thank Keith Putirka for the invitation that spurred the authors' collaboration on this
452 project, which was supported by the Geology Foundation of the University of Texas at Austin.

453 We are grateful for informal critiques by Ron Vernon and Greg Anderson, and for formal
454 reviews by Frank Spear and Sumit Chakraborty, all of which helped to shape and improve the
455 content and presentation of this article. WDC acknowledges support from NSF grant EAR-
456 1144309; DRMP acknowledges support from NSERC Discovery Grant 037233; and MJC
457 acknowledges support from NSF grant EAR-1250470.

458

REFERENCES CITED

- 459 Ague, J.J., and Carlson, W.D. (2013) Metamorphism as garnet sees it: The kinetics of nucleation
460 and growth, equilibration, and diffusional relaxation. *Elements*, 9, 439-445.
- 461 Austrheim, H. (1987) Eclogitization of lower crustal granulites by fluid migration through shear
462 zones. *Earth and Planetary Science Letters*, 81, 221-232.
- 463 Bell, T.H., and Hayward, N. (1991) Episodic metamorphic reactions during orogenesis — the
464 control of deformation partitioning on reaction sites and reaction duration. *Journal of*
465 *Metamorphic Geology*, 9, 619-640.
- 466 Caddick, M.J., and Kohn, M.J. (2013) Garnet: Witness to the evolution of destructive plate
467 boundaries. *Elements*, 9, 427-432.
- 468 Caddick, M.J., Konopasek, J., and Thompson, A.B. (2010) Preservation of garnet growth zoning
469 and the duration of prograde metamorphism. *Journal of Petrology*, 51, 2327-2347.
- 470 Carlson, W.D. (2002) Scales of disequilibrium and rates of equilibration during metamorphism.
471 *American Mineralogist*, 87, 185-204.
- 472 _____. (2011) Porphyroblast crystallization: Linking processes, kinetics, and
473 microstructures. *International Geology Review*, 53, 406-445.
- 474 Carlson, W.D., Hixon, J.D., Garber, J.M., and Bodnar, R.J. (2015) Controls on metamorphic
475 equilibration: The importance of intergranular solubilities mediated by fluid composition.
476 *Journal of Metamorphic Geology*, DOI: 10.1111/jmg.12113.
- 477 Carmichael, D.M. (1969) On the mechanism of prograde metamorphic reactions in quartz-
478 bearing pelitic rocks. *Contributions to Mineralogy and Petrology*, 20, 244-267.
- 479 de Donder, T. (1936) *Thermodynamic Theory of Affinity: A Book of Principles*. Oxford
480 University Press, Oxford.

- 481 Dragovic, B., Baxter, E.F., and Caddick, M.J. (in review) Pulsed dehydration and garnet growth
482 during subduction revealed by zoned garnet geochronology and thermodynamic
483 modeling, Sifnos, Greece. *Earth and Planetary Science Letters*.
- 484 Dragovic, B., Samanta, L.M., Baxter, E.F., and Selverstone, J. (2012) Using garnet to constrain
485 the duration and rate of water-releasing metamorphic reactions during subduction: An
486 example from Sifnos, Greece. *Chemical Geology*, 314, 9-22.
- 487 Gaidies, F., Pattison, D.R.M., and de Capitani, C. (2011) Toward a quantitative model of
488 metamorphic nucleation and growth. *Contributions to Mineralogy and Petrology*, 162,
489 975-993.
- 490 Greenwood, H.J. (1963) The synthesis and stability of anthophyllite. *Journal of Petrology*, 4,
491 317-351.
- 492 Groppo, C., Rolfo, F., and Lombardo, B. (2009) P-T evolution across the Main Central Thrust
493 Zone (Eastern Nepal): Hidden discontinuities revealed by petrology. *Journal of*
494 *Petrology*, 50, 1149-1180.
- 495 Kelly, E.D., Carlson, W.D., and Ketcham, R.A. (2013a) Crystallization kinetics during regional
496 metamorphism of porphyroblastic rocks. *Journal of Metamorphic Geology*, 31, 963-979.
- 497 _____. (2013b) Magnitudes of departures from equilibrium during regional
498 metamorphism of porphyroblastic rocks. *Journal of Metamorphic Geology*, 31, 981-1002.
- 499 Kerrick, D.M., Lasaga, A.C., and Raeburn, S.P. (1991) Kinetics of heterogeneous reactions.
500 *Reviews in Mineralogy*, 26, 583-671.
- 501 Ketcham, R.A., and Carlson, W.D. (2012) Numerical simulation of diffusion-controlled
502 nucleation and growth of porphyroblasts. *Journal of Metamorphic Geology*, 30, 489-512.

- 503 Konrad-Schmolke, M., O'Brien, P.J., De Capitani, C., and Carswell, D.A. (2007) Garnet growth
504 at high- and ultra-high pressure conditions and the effect of element fractionation on
505 mineral modes and composition. *Lithos*, 103, 309-332.
- 506 Konrad-Schmolke, M., Zack, T., O'Brien, P.J., and Jacob, D.E. (2008) Combined
507 thermodynamic and rare earth element modelling of garnet growth during subduction:
508 Examples from ultrahigh-pressure eclogite of the Western Gneiss Region, Norway. *Earth
509 and Planetary Science Letters*, 272, 488-498.
- 510 Martin, A.J. (2009) Sub-millimeter heterogeneity of yttrium and chromium during growth of
511 semipelitic garnet. *Journal of Petrology*, 50, 1713-1727.
- 512 Moore, S.J., Carlson, W.D., and Hesse, M.A. (2013) Origins of yttrium and rare-earth-element
513 distributions in metamorphic garnet. *Journal of Metamorphic Geology*, 31, 663-689.
- 514 Otamendi, J.E., de la Rosa, J.D., Patiño Douce, A.E., and Castro, A. (2002) Rayleigh
515 fractionation of heavy rare earths and yttrium during metamorphic garnet growth.
516 *Geology*, 30, 159-162.
- 517 Pattison, D.R.M., de Capitani, C., and Gaidies, F. (2011) Petrologic consequences of variations
518 in metamorphic reaction affinity. *Journal of Metamorphic Geology*, 29, 953-977.
- 519 Pattison, D.R.M., and Tinkham, D.K. (2009) Interplay between equilibrium and kinetics in
520 prograde metamorphism of pelites: An example from the Nelson aureole, British
521 Columbia. *Journal of Metamorphic Geology*, 27, 249-279.
- 522 Prigogine, I., and Defay, R.F. (1954) *Chemical Thermodynamics*. Longmans Green, London.
- 523 Putnis, A., and McConnell, J.D.C. (1980) *Principles of Mineral Behaviour*. Blackwell, Oxford,
524 257 p.

- 525 Pyle, J.M., and Spear, F.S. (1999) Yttrium zoning in garnet: Coupling of major and accessory
526 phases during metamorphic reactions. *Geological Materials Research*, 1, 1-49.
- 527 Ridley, J. (1986) Modelling of the relations between reaction enthalpy and the buffering of
528 reaction progress in metamorphism. *Mineralogical Magazine*, 50, 375-384.
- 529 Ridley, J., and Thompson, A.B. (1986) The role of mineral kinetics in the development of
530 metamorphic microtextures. In J.V. Walther and B.J. Wood, Eds. *Fluid-rock interactions*
531 *during metamorphism*, p. 154-193. Springer, New York Berlin Heidelberg Tokyo.
- 532 Rubie, D.C. (1986) The catalysis of mineral reactions by water and restrictions on the presence
533 of aqueous fluid during metamorphism. *Mineralogical Magazine*, 50, 399-415.
- 534 Rubie, D.C. (1998) Disequilibrium during metamorphism: The role of nucleation kinetics. In P.J.
535 Treloar and P.J. O'Brien, Eds. *What Drives Metamorphism and Metamorphic Reactions?*,
536 p. 199-214. Geological Society, London.
- 537 Schwarz, J.-O., Engi, M., and Berger, A. (2011) Porphyroblast crystallization kinetics: The role
538 of nutrient production rate. *Journal of Metamorphic Geology*, 29, 497-512.
- 539 Skora, S., Baumgartner, L.P., Mahlen, N.J., Johnson, C.M., Pilet, S., and Hellebrand, E. (2006)
540 Diffusion-limited REE uptake by eclogite garnets and its consequences for Lu–Hf and
541 Sm–Nd geochronology. *Contributions to Mineralogy and Petrology*, 152, 703-720.
- 542 Spear, F.S., and Daniel, C.G. (1998) Three-dimensional imaging of garnet porphyroblast sizes
543 and chemical zoning: Nucleation and growth history in the garnet zone. *Geological*
544 *Materials Research*, 1, 1-44.
- 545 Spear, F.S., Thomas, J.B., and Hallett, B.W. (2014) Overstepping the garnet isograd: A
546 comparison of QuiG barometry and thermodynamic modeling. *Contributions to*
547 *Mineralogy and Petrology*, 168-1059, 1-15.

- 548 Thompson, J.B., Jr. (1959) Local equilibrium in metasomatic processes. In P.H. Abelson, Ed.
549 Researches in Geochemistry, Vol. 1. Vol. 1, p. 427-457. Wiley, New York.
- 550 Tsujimori, T., Sisson, V.B., Liou, J.G., Harlow, G.E., and Sorensen, S.S. (2006) Petrologic
551 characterization of Guatemalan lawsonite eclogite: Eclogitization of subducted oceanic
552 crust in a cold subduction zone. In B.R. Hacker, W.C. McClelland and J.G. Liou, Eds.
553 Ultrahigh-pressure metamorphism: Deep continental subduction. Vol. 403, p. 147-168.
554 Geological Society of America, Boulder.
- 555 Walther, J.V., and Wood, B.J. (1984) Rate and mechanism in prograde metamorphism.
556 Contributions to Mineralogy and Petrology, 88, 246-259.
- 557 Waters, D.J., and Lovegrove, D.P. (2002) Assessing the extent of disequilibrium and
558 overstepping of prograde metamorphic reactions in metapelites from the Bushveld
559 Complex aureole, South Africa. Journal of Metamorphic Geology, 20, 135-149.
- 560 Yang, P., and Rivers, T. (2001) Chromium and manganese zoning in pelitic garnet and kyanite:
561 spiral, overprint, and oscillatory (?) zoning patterns and the role of growth rate. Journal of
562 Metamorphic Geology, 19, 455-474.
- 563
- 564

565

FIGURE CAPTIONS

566 **FIGURE 1. (a)** Sample locations (*dots*) and mapped isograds in the aureole of the Nelson
567 Batholith, British Columbia. *Solid lines*: mineral-in isograds. *Dashed lines*: mineral-out isograds.
568 **(b)** Predicted isograds from the same locality as (a), based on equilibrium thermodynamic
569 predictions and a modeled thermal profile. Diagrams and interpretations from Pattison and
570 Tinkham (2009).

571 **FIGURE 2.** Estimates of rate of build-up of macroscopic reaction affinity, due to thermal
572 overstepping of the equilibrium reaction position, for reactions of differing entropy. The uniform
573 energetic threshold for nucleation (*dotted line*) is used for comparative purposes only; in reality,
574 this will vary with the nature of mineral reactants/products and other factors. Diagram from
575 Pattison et al. (2011).

576 **FIGURE 3. (a)** Interpretation, based on microstructures, of the sequence of mineral growth
577 and consumption in porphyroblastic metapelites from the aureole of the Bushveld Intrusive
578 Complex, South Africa. **(b)** Predicted sequence of mineral growth and consumption in the same
579 rock as in (a), based on equilibrium thermodynamic predictions. **(c)** Interpreted overstepped
580 reaction interval involving several stable and metastable reactions occurring in parallel over a
581 narrow temperature range (cascade effect). The reaction sequence in (c) is the same as in (a), the
582 latter compressed into the estimated 540-560 °C thermal interval. Diagrams and interpretations
583 from, or based on, Waters and Lovegrove (2002).

584 **FIGURE 4.** Partial chemical equilibrium during garnet growth. (*left and center*) X-ray maps
585 of Mn and Cr concentrations, contrasting equilibrium drawdown of uniform Mn reservoir with
586 overprinting of Cr heterogeneities in matrix. After Yang and Rivers (2001). (*right*) Schematic
587 chemical-potential gradients in intergranular medium during growth of porphyroblast

588 (*rectangle*), for elements with fast (Mn), moderate (Al), and very slow (Cr) intergranular
589 diffusion.

590 **FIGURE 5.** Partial chemical equilibrium during garnet growth. X-ray maps of zoning
591 patterns in crystals *A*, *B*, and *C* display patchy overprint zoning of layered distributions of Mn,
592 Fe, and Mg, but smooth concentric zoning for Ca and Y. An immediately adjacent crystal *D*,
593 which grew in a mica-rich layer, exhibits smooth concentric zoning for all elements.

594 **FIGURE 6.** *P-T* diagram calculated for a blueschist-facies rock from Sifnos, Greece (rock
595 composition, thermodynamic data and mineral solution models as in Dragovic et al., 2012,
596 supplemented with an ideal solution model for Fe-Mg-Mn stilpnomelane). Color shading and
597 contours show increase in system free energy if garnet is excluded from the calculation, relative
598 to free energy if garnet is included. Contour interval is 100 J/mol of oxygen in garnet. *P-T*
599 regions in which an alternative porphyroblast-forming phase grows in place of garnet are shaded.
600 First recorded garnet compositions imply growth at *P-T* conditions significantly above
601 equilibrium stability for garnet-in. System free energy is lowered by ~ 0.5 kJ/mol of oxygen in
602 garnet if ~ 1 volume % garnet is grown at these *P-T* conditions.

603 **FIGURE 7.** Departures from equilibrium as computed by petrologically constrained
604 numerical simulation of diffusion-controlled nucleation and growth (details of calculations
605 appear in Kelly et al., 2013b). Along gray *P-T-t* path (*top*), initial nucleation of garnet is delayed
606 by 3 Ma to 27 °C above equilibrium *T*; bulk of garnet crystallization occurs 8-14 Ma after
607 reactants become unstable (*center, bottom*), and 50-80 °C above equilibrium boundary.
608 Computed delay in modal accumulation of garnet is consistent with measured systematic
609 correlations of crystal size with central composition (*insets at top*); last crystals to nucleate have
610 core compositions matching outer mantles of early-nucleating crystals, documenting that

611 nucleation persisted late into the crystallization interval, rather than being restricted to conditions
612 at or near the reaction boundary, as the equilibrium model requires.

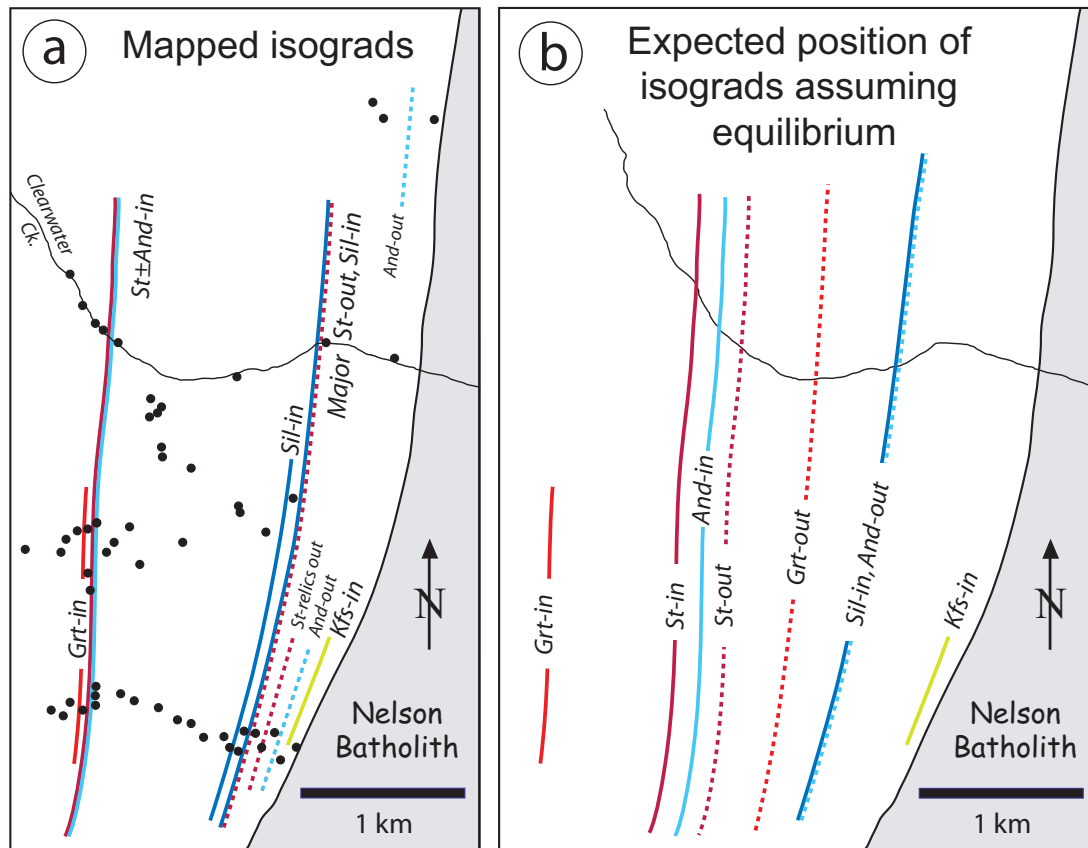


FIGURE 1

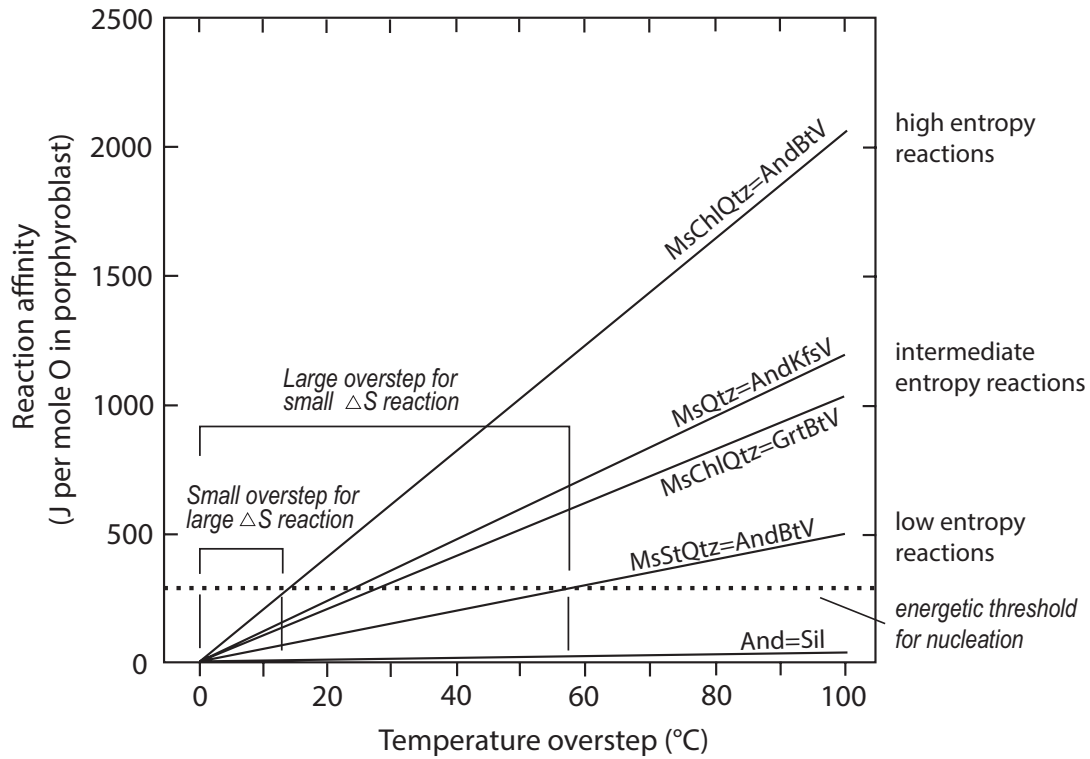
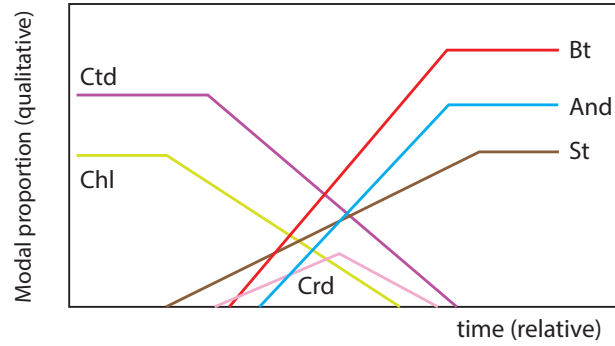
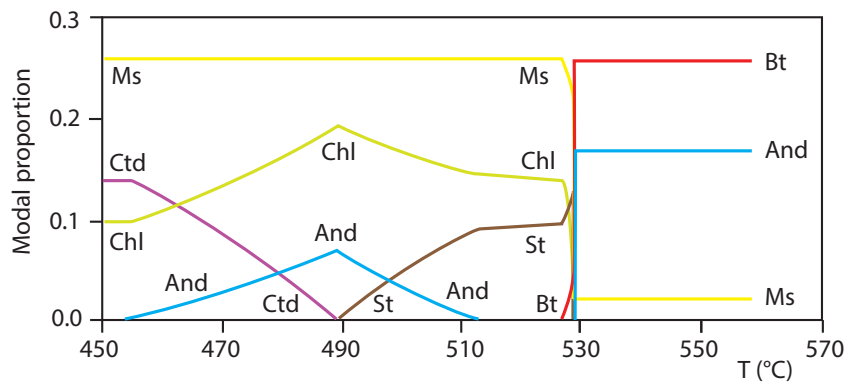


FIGURE 2

A. Qualitative mineral growth/consumption sequence from textures



B. Predicted mineral growth/consumption sequence (equilibrium)



C. Interpreted interval of overstepped mineral/growth consumption

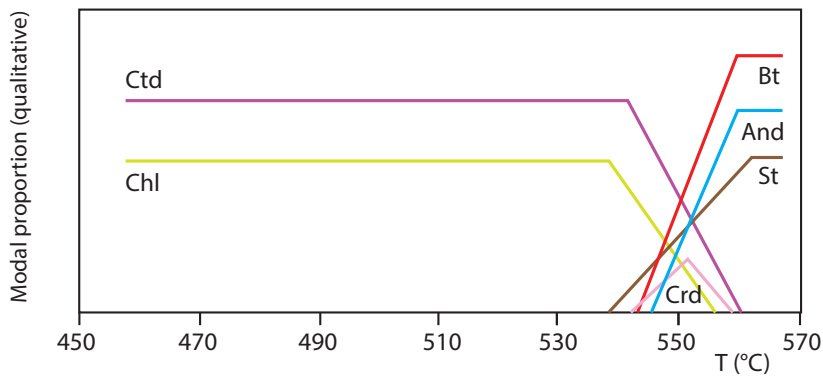


FIGURE 3

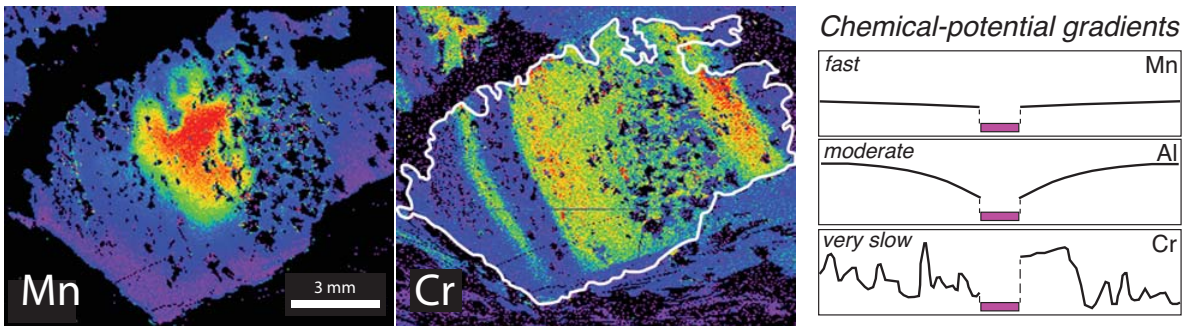


FIGURE 4

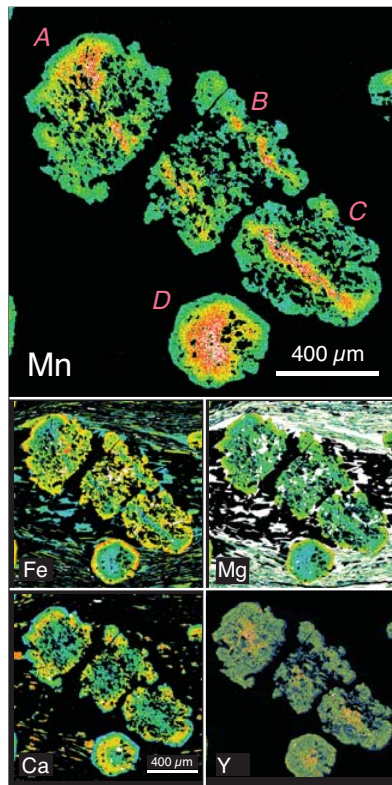


FIGURE 5

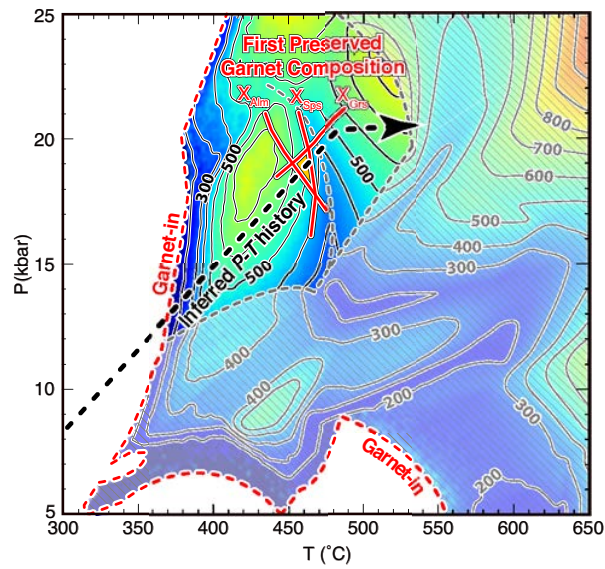


FIGURE 6

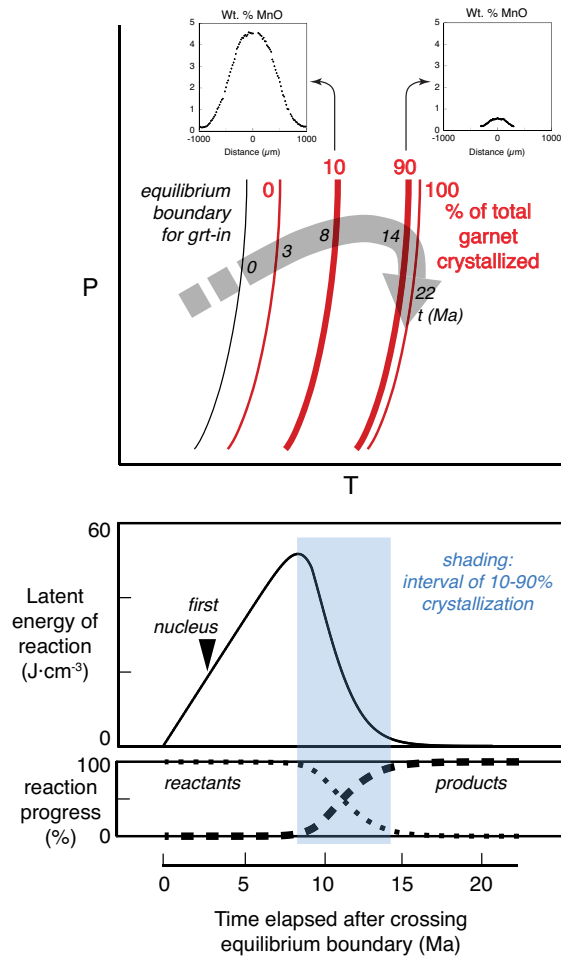


FIGURE 7